Supplementary Tables & Figures

Domain-general region overlap with the Cole-Anticevic brain-wide networks

To characterise these activations in relation to large-scale brain networks, we used a publicly available Cole-Anticevic brain-wide network partition (CAB-NP) (Ji et al., 2019). The CAB-NP was derived from resting-state fMRI data across the whole brain and used the Louvain community detection algorithm to assign parcellated cortical regions (Glasser et al., 2016) into 12 functional networks. We used the Connectome Workbench software (Marcus et al., 2011) to overlay our activations over the CAB-NP to estimate the parcel and network locations of our activation clusters.

For each estimated parcel we also identified its global variability coefficient (GVC), between-network variability coefficient (BVC) and network partition deviation numbers from Cocuzza et al. (2020) discovery and replication data sets. In Tables S1-S3 we present the identified parces for each of our activation clusters (Table 1 in the main text), their network assignment and center X, Y, Z coordinates, and GVC, BVC and deviation values averaged across Cocuzza et al. (2020) discovery and replication data sets. The top panels of Figures S1-S3 show our results clusters and estimated network assigments. Number of dots indicate to how many parcels within this network our cluster was assigned to. Dots were placed manually and are for the visualisation purposes only. The bottom panels show CAB-NP, our result maps in white and foci of our clusters. The foci were placed based on the MNI coordinates from the Table 1 of the main text.

Within-subjects Stop > Go & No-Think > Think conjunction clusters

Table S1

Parcel	Network	X	Y	Z	GVC	BVC	deviation	Parcel description
1. R VLPFC & Insula								
254	Frontoparietal	53	19	13	0.3469	0.3486	0.6563	R_Area_44
258	Cingular-Opercular	53	11	13	0.3534	0.3553	0.0000	R_Rostral_Area_6
288	Cingular-Opercular	39	16	6	0.3717	0.3721	0.8907	R_Frontal_Opercular_Area_4
289	Cingular-Opercular	38	13	1	0.3663	0.3691	0.1172	R_Middle_Insular_Area
291	Frontoparietal	33	26	-4	0.3289	0.3299	0.3204	R_Anterior_Ventral_Insular_Area
349	Cingular-Opercular	38	28	4	0.3714	0.3724	0.0078	R_Area_Frontal_Opercular
Mean					0.3564	0.3579	0.3321	
Cingular-Opercular					0.3657	0.3672	0.2539	
Frontoparietal					0.3379	0.3393	0.4884	
2. Right IPL								
205	Cingular-Opercular	63	-37	27	0.3789	0.3818	0.1797	R_PeriSylvian_Language_Area
208	Posterior Multimodal	57	-45	22	0.3609	0.3620	0.3282	R_Superior_Temporal_Visual_Area
328	Cingular-Opercular	60	-30	38	0.3443	0.3446	0.0000	R_Area_PF_Complex
329	Frontoparietal	51	-50	45	0.3351	0.3361	0.2501	R_Area_PFm_Complex
Mean					0.3548	0.3561	0.1895	
3. Right SMA								
206	Language	8	19	64	0.3794	0.3819	0.1954	R_Superior_Frontal_Language_Area
224	Cingular-Opercular	20	7	66	0.3463	0.3477	0.5079	R_Area_6m_anterior
278	Frontoparietal	20	25	57	0.3812	0.3831	1.0000	R_Superior_6-8_Transitional_Area
Mean					0.3690	0.3709	0.5678	
4. Right DLPFC								
264	Cingular-Opercular	36	41	30	0.3608	0.3625	0.0000	R_Area_46
266	Cingular-Opercular	29	50	22	0.3750	0.3770	0.0547	R_Area_9-46d
Mean					0.3679	0.3698	0.0274	
5. Right Precentral								
190	Cingular-Opercular	44	-2	51	0.3653	0.3667	0.0391	R_Frontal_Eye_Fields
191	Cingular-Opercular	47	3	37	0.3618	0.3625	0.0782	R_Premotor_Eye_Fields
192	Language	49	2	47	0.3996	0.4007	0.0078	R_Area_55b
253	Frontoparietal	40	18	36	0.3347	0.3357	0.0782	R_Area_IFJp

Mean					0.3654	0.3664	0.0508	
6. Left IPL								
148	Cingular-Opercular	-61	-36	36	0.3635	0.3653	0.6875	L_Area_PF_Complex
149	Frontoparietal	-50	-56	44	0.3767	0.3799	0.1094	L_Area_PFm_Complex
Mean					0.3701	0.3726	0.3985	

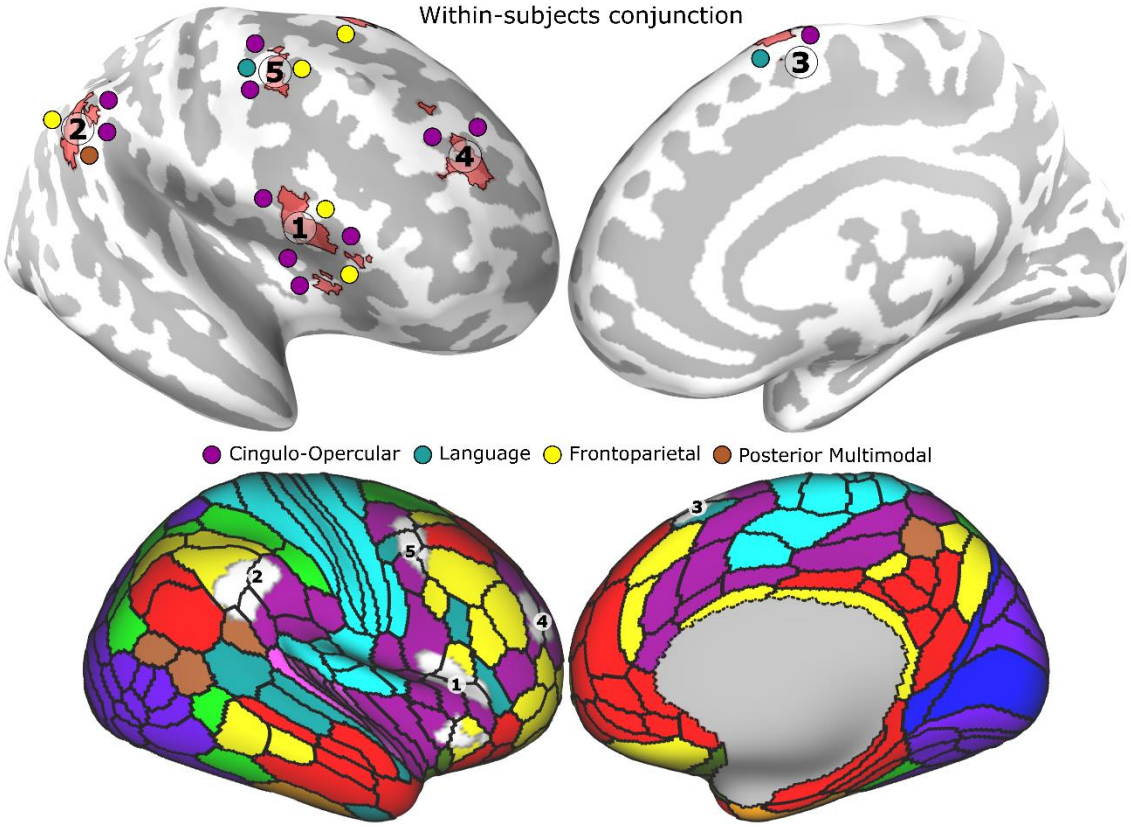

Figure S1

Meta-analysis Stop > Go & No-Think > Think conjunction clusters

Table S2

Parcel	Network	X	Y	Z	GVC	BVC	deviation	Parcel description
1. Right VLPFC & Insula								
254	Frontoparietal	53	19	13	0.3469	0.3486	0.6563	R_Area_44
288	Cingular-Opercular	39	16	6	0.3717	0.3721	0.8907	R_Frontal_Opercular_Area_4
289	Cingular-Opercular	38	13	1	0.3663	0.3691	0.1172	R_Middle_Insular_Area
291	Frontoparietal	33	26	-4	0.3289	0.3299	0.3204	R_Anterior_Ventral_Insular_Area
349	Cingular-Opercular	38	28	4	0.3714	0.3724	0.0078	R_Area_Frontal_Opercular
Mean					0.3570	0.3584	0.3985	
Cingular-Opercular					0.3698	0.3712	0.3386	
Frontoparietal					0.3379	0.3393	0.4884	
2. Right/Left SMA								
206	Language	8	19	64	0.3794	0.3819	0.1954	R_Superior_Frontal_Language_Area
223	Cingular-Opercular	6	6	58	0.3928	0.3951	0.0625	R_Supplementary_And_Cingulate_Eye
224	Cingular-Opercular	20	7	66	0.3463	0.3477	0.5079	R_Area_6m_anterior
243	Frontoparietal	5	32	46	0.3692	0.3698	0.2344	R_Area_8BM
278	Frontoparietal	20	25	57	0.3812	0.3831	1.0000	R_Superior_6-8_Transitional_Area
Mean					0.3738	0.3755	0.4000	
3. Left VLPFC & Insula								
109	Cingular-Opercular	-37	11	3	0.3519	0.3552	0.2422	L_Middle_Insular_Area
111	Frontoparietal	-31	25	-3	0.3805	0.3847	0.3438	L_Anterior_Ventral_Insular_Area
Mean					0.3662	0.3700	0.2930	
4. Right IPL								
205	Cingular-Opercular	63	-37	27	0.3789	0.3818	0.1797	R_PeriSylvian_Language_Area
208	Posterior Multimodal	57	-45	22	0.3609	0.3620	0.3282	R_Superior_Temporal_Visual_Area
328	Cingular-Opercular	60	-30	38	0.3443	0.3446	0.0000	R_Area_PF_Complex
329	Frontoparietal	51	-50	45	0.3351	0.3361	0.2501	R_Area_PFm_Complex

Mean					0.3548	0.3561	0.1895	
5. Right ACC								
239	Cingular-Opercular	4	19	32	0.3716	0.3705	0.8047	R_Anterior_24_prime
240	Cingular-Opercular	9	15	39	0.3795	0.3783	0.5782	R_Area_p32_prime
243	Frontoparietal	5	32	46	0.3692	0.3698	0.2344	R_Area_8BM
359	Cingular-Opercular	9	29	30	0.3592	0.3595	0.9922	R_Area_anterior_32_prime
Mean					0.3699	0.3695	0.6524	
6. Right DLPFC								
264	Cingular-Opercular	36	41	30	0.3608	0.3625	0.0000	R_Area_46
266	Cingular-Opercular	29	50	22	0.3750	0.3770	0.0547	R_Area_9-46d
Mean					0.3679	0.3698	0.0274	
7. Basal ganglia								
8. Left IPL								
148	Cingular-Opercular	-61	-36	36	0.3635	0.3653	0.6875	L_Area_PF_Complex
149	Frontoparietal	-50	-56	44	0.3767	0.3799	0.1094	L_Area_PFm_Complex
Mean					0.3701	0.3726	0.3985	
9. Right Precentral								
190	Cingular-Opercular	44	-2	51	0.3653	0.3667	0.0391	R_Frontal_Eye_Fields
192	Language	49	2	47	0.3996	0.4007	0.0078	R_Area_55b
Mean					0.3825	0.3837	0.0235	
10. Right SPL								
297	Dorsal Attention	38	-38	44	0.3888	0.3899	0.9610	R_Anterior_IntraParietal_Area
324	Frontoparietal	42	-42	46	0.3960	0.4011	0.2500	R_Area_IntraParietal_2
Mean					0.3924	0.3955	0.6055	

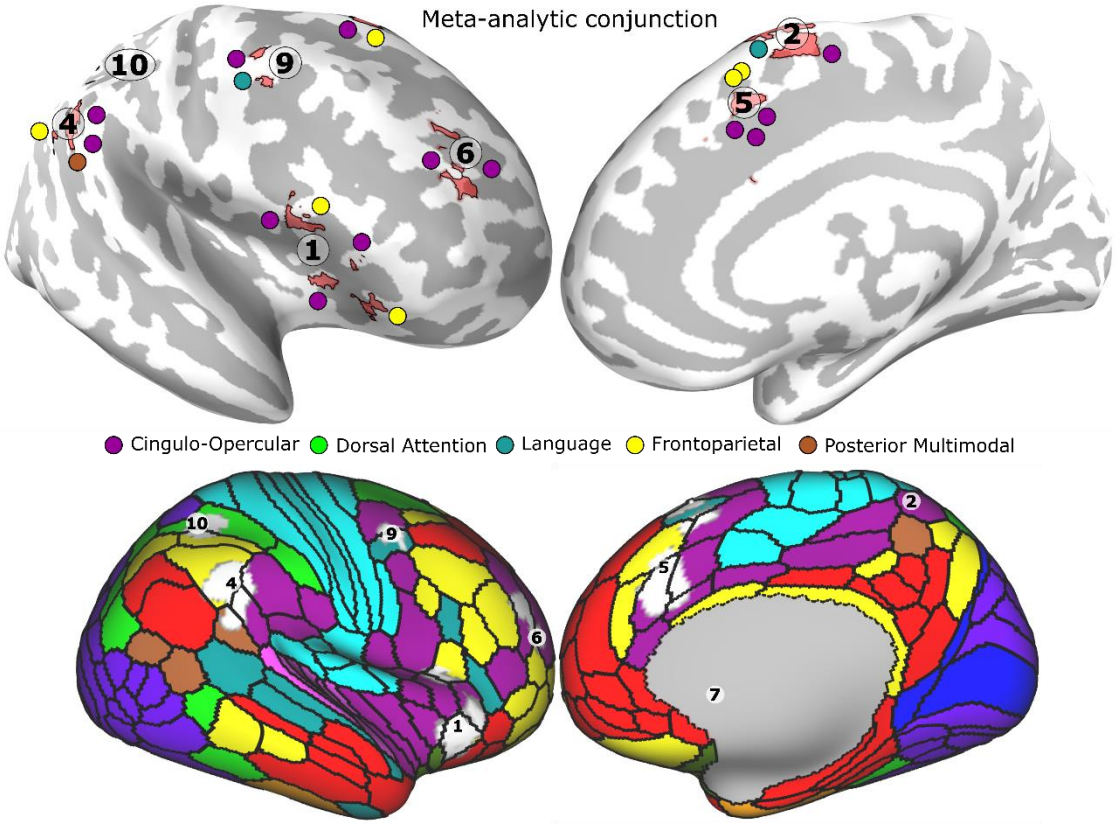

Figure S2

Conjunction of the within-subjects conjunction & meta-analysis conjuncion clusters

Table S3

Parcel	Network	X	Y	Z	GVC	BVC	deviation	Parcel description
1. Right VLPFC & Insula								
254	Frontoparietal	53	19	13	0.3469	0.3486	0.6563	R_Area_44
288	Cingular-Opercular	39	16	6	0.3717	0.3721	0.8907	R_Frontal_Opercular_Area_4
289	Cingular-Opercular	38	13	1	0.3663	0.3691	0.1172	R_Middle_Insular_Area
291	Frontoparietal	33	26	-4	0.3289	0.3299	0.3204	R_Anterior_Ventral_Insular_Area

349	Cingular-Opercular	38	28	4	0.3714	0.3724	0.0078	R_Area_Frontal_Opercular
Mean					0.3570	0.3584	0.3985	
Cingular-Opercular					0.3698	0.3712	0.3386	
Frontoparietal					0.3379	0.3393	0.4884	
2. Right IPL								
205	Cingular-Opercular	63	-37	27	0.3789	0.3818	0.1797	R_PeriSylvian_Language_Area
208	Posterior Multimodal	57	-45	22	0.3609	0.3620	0.3282	R_Superior_Temporal_Visual_Area
328	Cingular-Opercular	60	-30	38	0.3443	0.3446	0.0000	R_Area_PF_Complex
329	Frontoparietal	51	-50	45	0.3351	0.3361	0.2501	R_Area_PFm_Complex
Mean					0.3548	0.3561	0.1895	
3. Right SMA								
206	Language	8	19	64	0.3794	0.3819	0.1954	R_Superior_Frontal_Language_Area
278	Frontoparietal	20	25	57	0.3812	0.3831	1.0000	R_Superior_6-8_Transitional_Area
224	Cingular-Opercular	20	7	66	0.3463	0.3477	0.5079	R_Area_6m_anterior
Mean					0.3690	0.3709	0.5678	
4. Right DLPFC								
264	Cingular-Opercular	36	41	30	0.3608	0.3625	0.0000	R_Area_46
266	Cingular-Opercular	29	50	22	0.3750	0.3770	0.0547	R_Area_9-46d
Mean					0.3679	0.3698	0.0274	
5. Left IPL								
148	Cingular-Opercular	-61	-36	36	0.3635	0.3653	0.6875	L_Area_PF_Complex
149	Frontoparietal	-50	-56	44	0.3767	0.3799	0.1094	L_Area_PFm_Complex
Mean					0.3701	0.3726	0.3985	
6. Right Precentral								
190	Cingular-Opercular	44	-2	51	0.3653	0.3667	0.0391	R_Frontal_Eye_Fields
192	Language	49	2	47	0.3996	0.4007	0.0078	R_Area_55b
Mean					0.3825	0.3837	0.0235	

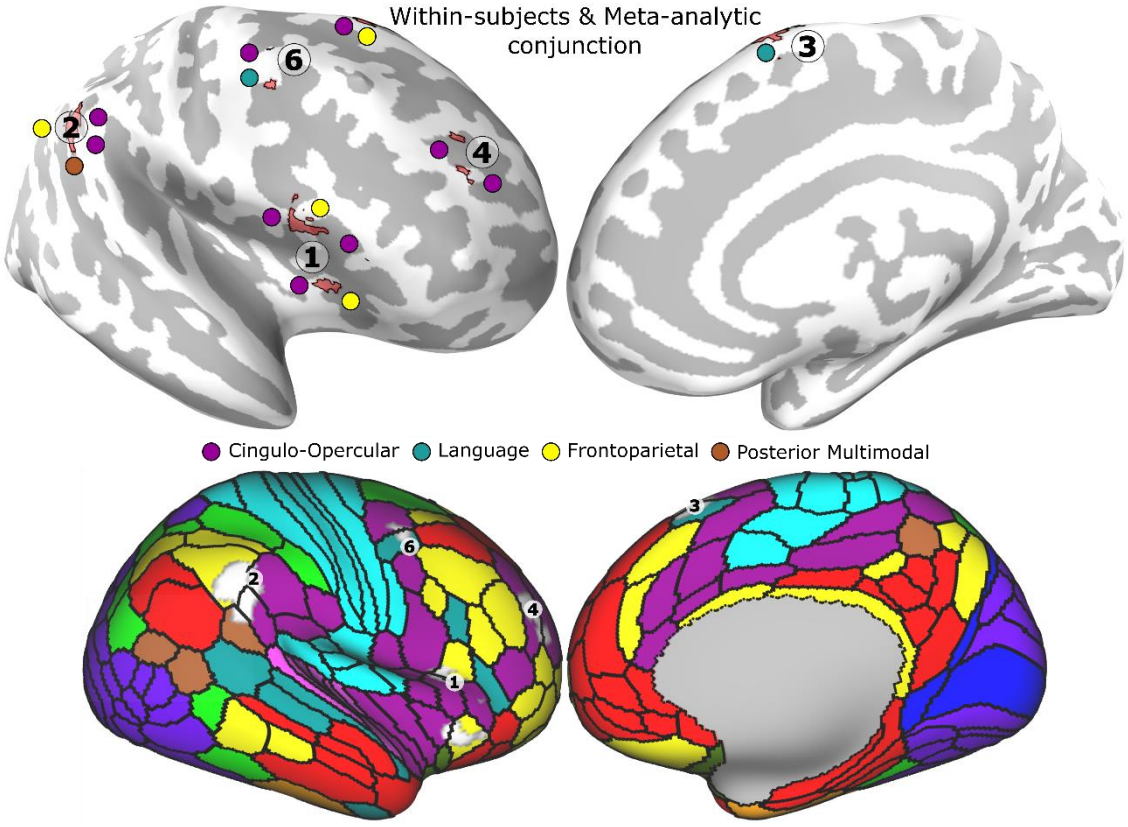

Figure S3

Conflict reduction

Figures S4A and S5A show how accurately a classifier trained to distinguish Stop from Go conditions, classifies No-Think as Stop condition for each of the 8 fMRI task runs in the rDLPFC and rVLPFC, respectively.

Figures S4B and S5B show correlation between the suppression induced forgetting (SIF) and slope of the classification accuracy over runs (measured as the accuracy slope divided by the accuracy of the first run), in the rDLPFC and rVLPFC, respectively.

Figures S4C and S5C show correlation between the stop-signal reaction time (SSRT) and slope of the classification accuracy over runs, in the rDLPFC and rVLPFC, respectively.

rDLPFC

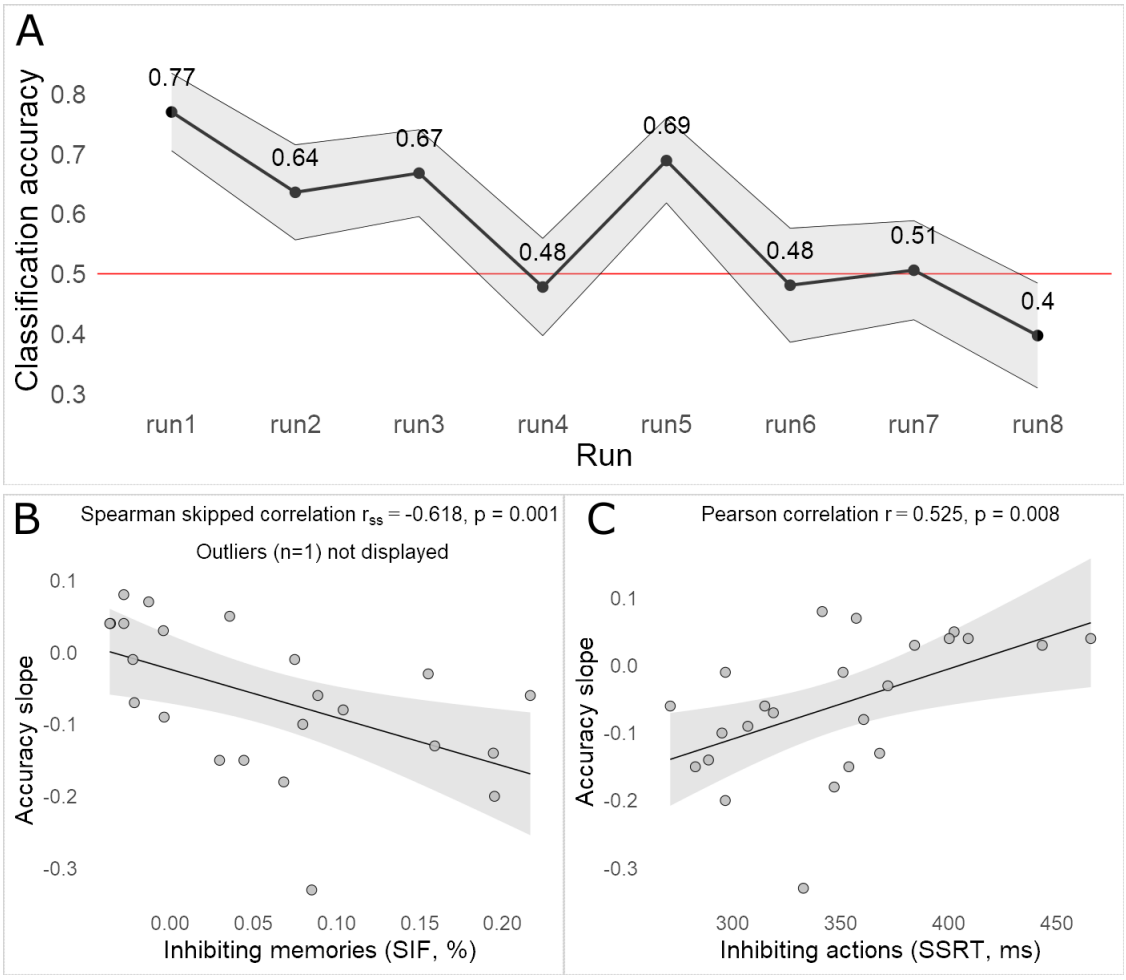

Figure S4

rVLPFC

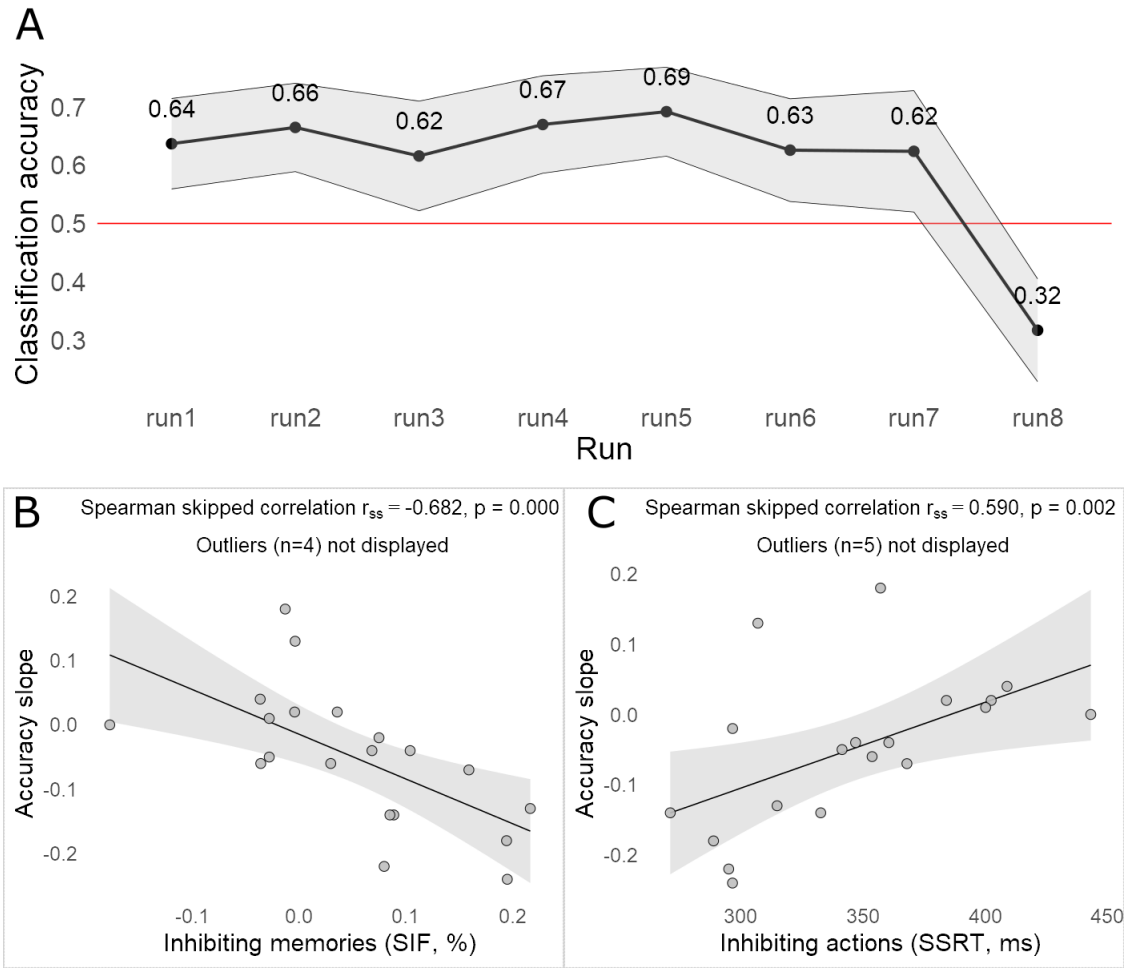

Figure S5.

References

Cocuzza C V, Ito T, Schultz D, Bassett DS, Cole MW (2020) Flexible coordinator and switcher hubs for adaptive task control. *bioRxiv* doi:10.1101/822213.

Glasser MF, Coalson TS, Robinson EC, Hacker CD, Harwell J, Yacoub E, Ugurbil K, Andersson J, Beckmann CF, Jenkinson M, Smith SM, Van Essen DC (2016) A multi-modal parcellation of human cerebral cortex. *Nature* 536:171–178 doi:10.1038/nature18933.

Ji JL, Spronk M, Kulkarni K, Repovš G, Anticevic A, Cole MW (2019) Mapping the human brain's cortical-subcortical functional network organization. *NeuroImage* 185:35–57 doi:10.1016/j.neuroimage.2018.10.006.

Marcus DS, Harwell J, Olsen T, Hodge M, Glasser MF, Prior F, Jenkinson M, Laumann T, Curtiss SW, Van Essen DC (2011) Informatics and data mining tools and strategies for the human connectome project. *Frontiers in Neuroinformatics* 5:1–12 doi:10.3389/fninf.2011.00004.